

# FINAL-FOCUS OPTICS FOR THE LHeC ELECTRON BEAM LINE\*

J.L. Abelleira<sup>1,2</sup>, H. Garcia<sup>1,3</sup>, R Tomas<sup>1</sup>, F. Zimmermann<sup>1</sup>

<sup>1</sup>CERN, Geneva, Switzerland; <sup>2</sup>EPFL, Lausanne, Switzerland; <sup>3</sup>UPC, Barcelona, Spain

## Abstract

One of the options considered for the ECFA-CERN-NuPECC design study for a Large Hadron electron Collider (LHeC) [1] based on the LHC is adding a recirculating energy-recovery linac tangential to the LHC. First designs of the electron Final Focus System have shown the need to correct the chromatic aberrations. Two designs using different approaches for the chromaticity correction are compared, namely, the local chromaticity correction [2] and the traditional approach using dedicated sections.

## INTRODUCTION

The LHeC will provide simultaneous pp and ep collisions. The electron beam will collide at 60 GeV with the proton one in LHC Interaction Point (IP) 2. In the linac-ring option, the electron beam will be deflected before and after the collision point with weak dipole magnets positioned in front of the superconducting final quadrupole triplets of the 7 TeV proton beam. A first proposal for the lepton optics is also made in [2], where two Final Focus (FF) are presented. In order to obtain the high design luminosity of  $L = 10^{33} \text{ cm}^{-2}\text{s}^{-1}$  with an average lepton beam current of 6 mA, the beam size growth due to the momentum spread must be minimized. Here two new conceptual designs based on two different approaches are presented, improving the chromatic correction in [2], with larger systems. The values for the IP beta functions considered are  $\beta_x^* = 2 \text{ m}$  and  $\beta_y^* = 0.05 \text{ m}$ . For the electron beam, a normalized emittance of  $\epsilon_N = 6 \mu\text{m}$  and a momentum spread of  $\sigma_\delta = 0.3 \times 10^{-3}$  are assumed.

## CHROMATIC CORRECTION

Considering a final-focus (FF) system consisting of ideal quadrupole magnets only, for a beam of nominal energy with zero momentum spread, the spot size at the IP is  $\sigma^* = \sqrt{\epsilon\beta^*}$ . When an spread  $\sigma_\delta$  is considered, the beam size is diluted by the chromaticity of the strong lenses which form the final doublet (FD). This chromaticity scales approximately as  $\xi \sim (L^* + L_q/2)/\beta^*$ , where  $L^*$  is the distance from the IP to the last quadrupole and  $L_q$  is the length of the last quadrupole. The design of the final focus is driven primarily by the necessity of compensating the chromaticity of the FD.

There are two different approaches to compensate the chromatic effect, which we call the traditional scheme and the local correction scheme.

## Traditional Scheme

The traditional FF system is of modular construction: The chromaticity is compensated in two dedicated sections, each of which corrects the chromaticity in one plane. The separated optics with strictly defined functions makes the system relatively simple to design. However, as the chromaticity is not locally corrected the bandwidth of the system is limited by the off-momentum breakdown of the proper relations between the sextupoles and the FD.

## Local Correction Scheme

An alternative solution addressing the aforementioned problem was proposed in [3]. The basic idea is to perform the FD chromatic correction locally, by placing the sextupoles next to the FD. The locally corrected system can be much shorter in length and the bandwidth significantly higher than for the traditional scheme. Since the correction of the FD chromaticity does not require the “transport of the sextupole kicks” over several (many) quadrupoles, the generation of bandwidth-limiting higher-order chromogeometric aberrations is minimized.

## FF WITH LOCAL CORRECTION

The system is 150 m long and consists of two focusing and two defocusing quadrupoles. Figure 1 presents the layout of the lattice and an optics plot for the  $\beta$ -functions and the dispersion. Two pairs of sextupoles are placed at every peak of the  $\beta$ -function, next to the quadrupoles. Bending dipoles generate the dispersion needed in the final doublet to correct chromaticity. These bending magnets, which are longer and weaker than those of the FF shown in [2], result in a SR power of 83 kW (mostly in the final 9-m long 0.3-T separation dipole near the IP which is common to all LHeC FF designs).

The compensation of the chromatic aberrations is illustrated in Fig. 2, where the beam size is calculated at different Taylor-map orders both for a monochromatic beam and for a Gaussian beam with  $\sigma_\delta = 0.3 \times 10^{-3}$ . The difference at orders 1 (linear) and 2 (quadratic) is due to the sextupoles. It is small because of the compensation of the geometric aberrations. The beam-size values shown must be compared with those obtained without any chromatic correction, which are  $\sigma_x^* = 11.64 \mu\text{m}$ ,  $\sigma_y^* = 6.08 \mu\text{m}$ .

## TRADITIONAL FF SYSTEM

In this case the system is about 267 m long and consists a two dedicated chromatic correction sections and a final transformer containing the FD. Four bending sections create and correct the dispersion needed for the chromatic

\* Work supported in part by the European Commission under the FP7 Research Infrastructures project EuCARD, grant agreement no. 227579.

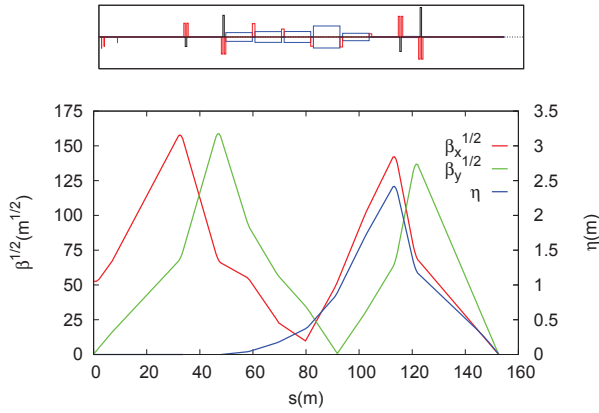


Figure 1: FF optics with local chromatic correction.

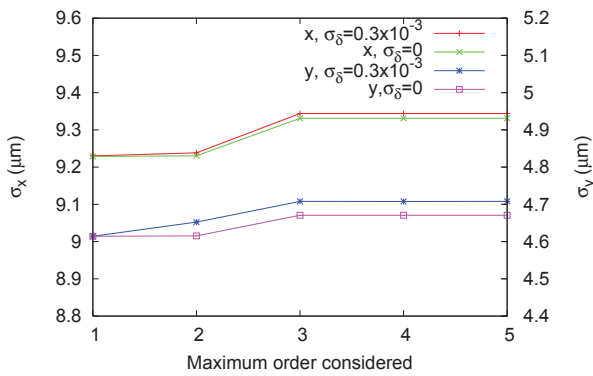


Figure 2: Beam size for order considered computed by MAPCLASS [4] for the FF with local chromatic correction.

correction. These sections are long and weak generating a synchrotron radiation power of 39 kW, much lower than in the local correction scheme. Figure 3 shows the layout of the system together with a plot of the  $\beta$ -functions and the dispersion.

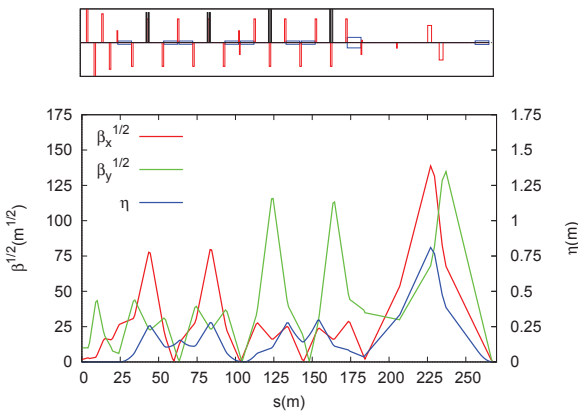


Figure 3: Layout of the FFS with dedicated chromatic correction sections.

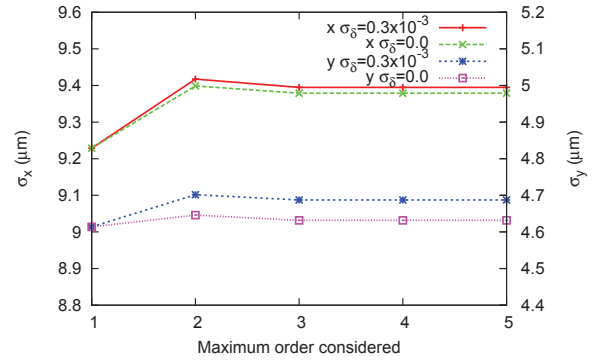


Figure 4: Beam size for order considered computed by MAPCLASS for the FF with dedicated chromatic correction sections.

The compensation of the chromatic effects is illustrated in Fig. 4, where as before we show beam sizes computed order by order for a beam with a Gaussian energy distribution of  $\sigma_\delta = 0.3 \times 10^{-3}$ .

## COMPARISON

### Beam Size and Tracking

In Table 1 we list the beam sizes obtained by particle tracking with PLACET. The numbers are consistent with the analytical calculation using MAPCLASS [4] and also with MADX tracking. In the absence of synchrotron radiation, the local correction scheme presents smaller beam spot sizes.

Table 1: Horizontal and vertical beam size for a beam with momentum spread  $\sigma_\delta = 0.3 \times 10^{-3}$  without synchrotron radiation evaluated by tracking with PLACET.

Scheme	$\sigma_x$ [ $\mu\text{m}$ ]	$\sigma_y$ [ $\mu\text{m}$ ]
Local	9.34	4.69
Traditional	9.75	4.97

### Synchrotron Radiation Effects

One of the main limitations of the beam size at the IP is the synchrotron radiation emitted in the bending magnets of the FF system. Here we compare the radiation emitted for both schemes and its effect on the emittance growth and the resulting IP beam-size blow up.

The dilution of the horizontal IP beam size due to synchrotron radiation can be estimated from [5]

$$\Delta \left( \sigma_x^{*2} / \beta_x^* \right) = 4.13 \times 10^{-11} \text{m}^2 \text{GeV}^{-5} E^5 \mathcal{I} \quad (1)$$

where  $E$  is the beam energy and  $\mathcal{I}$  is the integral

$$\mathcal{I} = \int_0^L \frac{\mathcal{H}(s)}{|\rho_x(s)^3|} \cos^2 \Phi(s) ds \approx \sum_i L_i \frac{\mathcal{H}_i}{\rho_{x,i}^3} \cos^2 \Phi_i \quad (2)$$

where  $L_i$  and  $\rho_i$  denotes the length and the bending radius of the  $i$  dipole magnet, and  $\mathcal{H}$  is defined as

$$\mathcal{H} = \frac{D_x^2 + (D'_x \beta_x + D_x \alpha_x)^2}{\beta_x} \quad (3)$$

with  $\Phi = \Delta\phi_x(s \rightarrow L) + \arctan(-\alpha_x - \beta D'_x/D_x)$ , and  $\phi_x$  the betatron phase advance.

The approximation in (2) of the integral by a sum can be used if the bending magnets are split into sufficiently short portions.

Table 2 compares the horizontal IP beam sizes with and without synchrotron radiation obtained from tracking simulations with the code PLACET and the analytical estimate from Eq. (2).

Table 2: Synchrotron radiation effects due to emittance dilution in the horizontal plane. Numbers in the two first columns were computed by tracking and those in the third estimated using (2).

Scheme	$\sigma_x$ [ $\mu\text{m}$ ] w/o synch.	$\sigma_x$ [ $\mu\text{m}$ ] w synch.	$\sigma_x$ [ $\mu\text{m}$ ] expected
Local	9.41	22.24	22.33
Traditional	10.15	12.84	13.63

We observe that the influence of the synchrotron radiation is more dramatic in the local correction scheme. This is due mainly to the fact that the dipole length and field are not optimized and they are located in regions where the behaviour of the Twiss functions in (3) makes  $\mathcal{H}$  larger than in the case of the traditional final focus scheme, where the Twiss functions are more relaxed in the bending sections. Although, as we have seen, the chromatic correction in the traditional scheme is not perfect due to the weaker bending magnets, the overall result looks better.

### Bandwidth

The performance of the FF with respect to small variations in the beam energy is characterized by the momentum bandwidth. For the local correction scheme a better bandwidth is expected [3]. The bandwidth of the FF with local chromatic corrections is shown Fig. 5, the one for the traditional system in Fig. 6. Comparing these two figures, the beam-size growth due to an energy offset ( $\beta^*$  vs  $\delta \equiv \Delta p/p$ ) and due to an energy spread ( $\sigma_{x,y}^*$  vs  $\sigma_\delta$ ) indeed are much larger for the modular system than for the locally corrected one.

## CONCLUSIONS

Two LHeC L-R FF alternatives have been added to those presented in [2]. The two systems explore two different chromatic corrections. The local approach is more compact and exhibits a much larger bandwidth. However the horizontal beam-size increase due to SR emitted in bending magnets is considerably higher. In the future, we plan

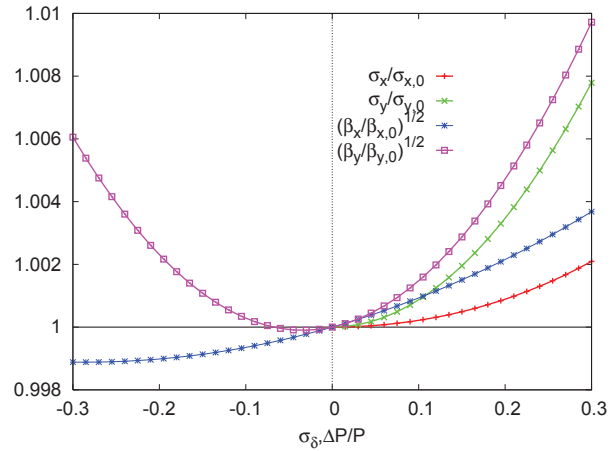


Figure 5: IP bandwidth of the local FFS. Normalized betatron functions versus energy offset and normalized beam size (determined by MAPCLASS) versus energy spread  $\sigma_\delta$ .

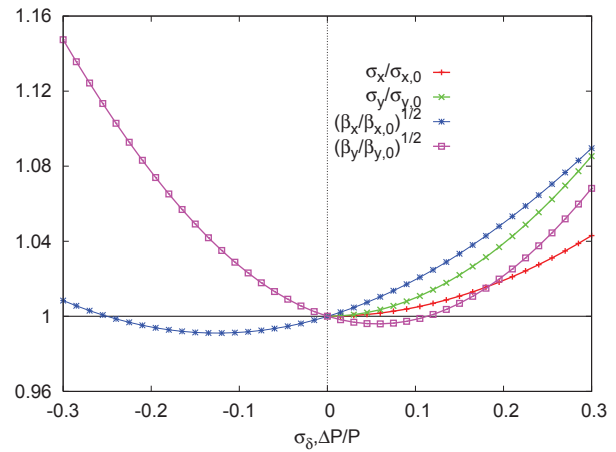


Figure 6: IP bandwidth of the dedicated section FFS. Normalized betatron functions versus energy offset and normalized beam size (determined by MAPCLASS) versus energy spread  $\sigma_\delta$ .

to further optimize the performance of the compact system by adjusting the bending magnets so as to minimize Eq. (2).

## REFERENCES

- [1] LHeC Study Group, C. Adolphsen et al, LHeC-Note-2011-003 GEN, CERN, 2011, to be published.
- [2] J.L. Abelleira et al, Proc. IPAC'11 San Sebastian, p. 2796.
- [3] P. Raimondi, A. Seryi, PRL 86, 3779 (2001).
- [4] R. Tomas, CERN AB-Note-2006-017 (ABP) (2006).
- [5] M. Sands, SLAC/AP-047 (1985).